



# Mapping Critical Language Sites in Children Performing Verb Generation: Whole-Brain Connectivity and Graph Theoretical Analysis in MEG

Vahab Youssofzadeh<sup>1,2</sup>, Brady J. Williamson<sup>1,3</sup> and Darren S. Kadis<sup>1,2,4\*</sup>

<sup>1</sup>Pediatric Neuroimaging Research Consortium (PNRC), Cincinnati Children's Hospital Medical Center, Cincinnati, OH, USA, <sup>2</sup>Division of Neurology, Cincinnati Children's Hospital Medical Center, Cincinnati, OH, USA, <sup>3</sup>Department of Psychology, University of Cincinnati, Cincinnati, OH, USA, <sup>4</sup>College of Medicine, Department of Pediatrics, University of Cincinnati, Cincinnati, OH, USA

A classic left frontal-temporal brain network is known to support language processes. However, the level of participation of constituent regions, and the contribution of extra-canonical areas, is not fully understood; this is particularly true in children, and in individuals who have experienced early neurological insult. In the present work, we propose whole-brain connectivity and graph-theoretical analysis of magnetoencephalography (MEG) source estimates to provide robust maps of the pediatric expressive language network. We examined neuromagnetic data from a group of typically-developing young children ( $n = 15$ , ages 4–6 years) and adolescents ( $n = 14$ , 16–18 years) completing an auditory verb generation task in MEG. All source analyses were carried out using a linearly-constrained minimum-variance (LCMV) beamformer. Conventional differential analyses revealed significant ( $p < 0.05$ , corrected) low-beta (13–23 Hz) event related desynchrony (ERD) focused in the left inferior frontal region (Broca's area) in both groups, consistent with previous studies. Connectivity analyses were carried out in broadband (3–30 Hz) on time-course estimates obtained at the voxel level. Patterns of connectivity were characterized by *phase locking value* (PLV), and network hubs identified through *eigenvector centrality* (EVC). Hub analysis revealed the importance of left perisylvian sites, i.e., Broca's and Wernicke's areas, across groups. The hemispheric distribution of frontal and temporal lobe EVC values was asymmetrical in most subjects; left dominant EVC was observed in 20% of young children, and 71% of adolescents. Interestingly, the adolescent group demonstrated increased critical sites in the right cerebellum, left inferior frontal gyrus (IFG) and left putamen. Here, we show that whole brain connectivity and network analysis can be used to map critical language sites in typical development; these methods may be useful for defining the margins of eloquent tissue in neurosurgical candidates.

**Keywords:** magnetoencephalography, hubs, eigenvector centrality, expressive language, verb generation, graph theory, connectivity, phase locking value

## OPEN ACCESS

### Edited by:

Vladimir Litvak,  
UCL Institute of Neurology, UK

### Reviewed by:

Fahimeh Mamashli,  
MGH/HST Martinos Center for  
Biomedical Imaging, USA  
Hyojin Park,  
University of Glasgow, UK

### \*Correspondence:

Darren S. Kadis  
darren.kadis@cchmc.org

**Received:** 31 January 2017

**Accepted:** 22 March 2017

**Published:** 05 April 2017

### Citation:

Youssofzadeh V, Williamson BJ and  
Kadis DS (2017) Mapping Critical  
Language Sites in Children  
Performing Verb Generation:  
Whole-Brain Connectivity and Graph  
Theoretical Analysis in MEG.  
Front. Hum. Neurosci. 11:173.  
doi: 10.3389/fnhum.2017.00173

## INTRODUCTION

Neuroimaging studies using functional magnetic resonance imaging (fMRI) and magnetoencephalography (MEG) have consistently identified a left-lateralized frontal-temporal functional network for language processing in the vast majority of right-handed adults (~95%; Binder et al., 1997; Gabrieli et al., 1998; Price, 2000; Hirata et al., 2004; Lohmann et al., 2010; Friederici, 2011, 2012; Kadis et al., 2011; Pei et al., 2011; Turken and Dronkers, 2011). The network includes Broca's area, in the posterior convolutions of the left inferior frontal gyrus (IFG; see Broca, 1861), and Wernicke's area in the posterior left superior temporal gyrus (STG; Wernicke, 1874) responsible for *expressive* and *receptive* language processes, respectively. Developmental language studies have reported similar frontal-temporal network for children, but with decreased lateralization and increased engagement beyond the canonical language network (Holland et al., 2007; Karunanayaka et al., 2007; Kadis et al., 2011; Berl et al., 2014). Active involvement of subcortical and cerebellar regions have also been reported in imaging studies (Frings et al., 2006; Booth et al., 2007; Houk et al., 2007; Murdoch, 2010; Berl et al., 2014; Verly et al., 2014). However, the level of participation of constituent regions, and the contribution of extra-canonical areas, is not fully understood; this is particularly true for pediatrics, and in individuals who have experienced early neurological insult.

More recently, researchers have begun to use sophisticated analytic strategies such as functional and effective connectivity analysis to explore regional interactions for language (Bitan et al., 2005, 2006; Sonty et al., 2007; Allen et al., 2008; Leff et al., 2008; Schofield et al., 2009; David et al., 2011; Doesburg et al., 2012, 2015; Verly et al., 2014; Kadis et al., 2015; Xiao et al., 2016). In our recent MEG study of verb generation in children, we observed frequency dependent patterns of connectivity together with an increased number of suprathreshold effective (directed) connections with age, even though the extent of the network decreased and became increasingly left lateralized with age (Kadis et al., 2015). Others have used dynamic causal modeling (DCM) in fMRI to show that higher level language processing is relatively left lateralized, compared to basic sensory processes (Bitan et al., 2005, 2006; Sonty et al., 2007; Allen et al., 2008; Cao et al., 2008; Leff et al., 2008; Schofield et al., 2009; Xiao et al., 2016). In addition, involvement of subcortical structures in language processing has been supported by DCM for MEG and fMRI data related to auditory comprehension task (Booth et al., 2007; David et al., 2011). However, these studies have mainly focused on interactions of distinct nodal regions (seeds) or limited prespecified regions of interest (ROIs). In the case of DCM, a clear hypothesis regarding the directionality of coupling and network architecture is also required. As a result, the complexity of the brain network controlling language has remained largely unresolved with neuroimaging.

Graph theoretical measures are increasingly used to reveal non-trivial characteristics of human brain networks, including functional integration (summary statistics of broad connectivity patterns) and segregation (the identification of specialized

regions or local groups; Rubinov and Sporns, 2010). The importance of a particular node may be determined by the amount or quality of its connectedness (where highly connection nodes are termed "hubs"; He and Evans, 2010; McIntosh and Mišić, 2013; Power et al., 2013; Fornito et al., 2015; Fuertinger et al., 2015). Investigating hubs can help to answer questions of how complex networks might develop, or how networks are altered in neuropsychiatric disease, such as Alzheimer's or schizophrenia (Achard and Bullmore, 2007; Bassett et al., 2009; Stam et al., 2009; Supekar et al., 2009; Mandelli et al., 2016).

Here, we propose whole-brain connectivity and graph-theoretical analysis of task-related MEG source estimates to provide robust maps of the pediatric expressive language network. We quantify voxel-level connectivity using the *phase locking value* (PLV) metric (Lachaux et al., 1999) and network hubs via three graph metrics: *degree*, *eigenvector centrality* (EVC) and *betweenness centrality* (Rubinov and Sporns, 2010). We employ automated parcellation to summarize voxel-level connectivity findings as they relate to age.

## MATERIALS AND METHODS

### Participants and Experiment Design

Two groups of subjects were recruited for this study: 15 typically-developing young children (8 females, aged 4–6 years, mean  $\pm$  SD:  $5.6 \pm 0.94$ ) and 14 adolescents (8 females, aged 16–18,  $17.18 \pm 0.79$ ). Participants were recruited from the community (Cincinnati), through flyers and online advertisements. All were native English speakers without history of neurological insult, speech or language disorder, or learning disability; all scanning was conducted for the sole purpose of research participation. This study was carried out in accordance with the recommendations of title 45, part 46, and title 21 parts 50 and 56, of the Code of Federal Regulations, with written informed consent from all subjects. All subjects gave written informed consent or parental consent and child assent were obtained in all cases in accordance with the Declaration of Helsinki. The study was approved by the Institutional Review Board (IRB) at Cincinnati Children's Hospital Medical Center. Participants received compensation for travel and participation.

Subjects completed a covert auditory verb generation MEG experiment. Target stimuli were auditorily presented and subjects were instructed to rapidly think of an action word that corresponded to the presented noun. Items were chosen from normative databases and standardized language assessments; each item and its usage were familiar to typically-developing 5-year old children, (e.g., book, dog, pencil). Development of the stimulus set has been described previously (Kadis et al., 2011). Prior to the MEG recording, participants were trained on an overt version of the task in order to establish sufficient ability and promote compliance during subsequent acquisition.

The control task involved passive listening to noise stimuli (contoured noise, matched to target stimuli in terms of spectral

content and amplitude envelope). Target and noise stimuli were identical in duration ( $0.67 \pm 0.14$  s), presented alternately, once every 4–5 s (range reflects random jitter). A total of 71 distinct nouns and 71 noise trials were presented. Since we were interested in verb generation (expressive language), we focused on responses to nouns only.

## Data Acquisition

Participants underwent MEG, MRI, fMRI and diffusion imaging in this study; only MEG and structural MRI are analyzed, here. MEG data were acquired using a whole-head 275-channel CTF system (MEG International Services Ltd., Coquitlam, BC, Canada) with a sampling rate of 1.2 kHz. All participants were tested in a supine position with their heads supported on memory foam and linens for comfort and stability. We limited the duration of scanning to less than 20 min of acquisition (total, across all MEG paradigms), to minimize fatigue and disinterest. Stimuli were presented via a calibrated audio system comprised of a distal transducer, tubing and ear inserts (Etymotic Research, IL, USA). Head localization coils were placed at nasion and preauricular points to monitor movement. In all cases, head displacement was less than 5 mm from the beginning to end of acquisition. To facilitate MEG coregistration, multimodal radiographic markers were placed at the same fiducial locations before acquiring structural images.

MRI was conducted at 3.0T on a Philips Achieva scanner (Philips Medical Systems) located at Cincinnati Children's Hospital Medical Center. A whole brain 3D T1-weighted image was acquired using an MDEFT scan (flip angle =  $90^\circ$ , TE = 3.7 ms, TR = 8.1 ms, TI = 939 ms, voxel size =  $1.0 \times 1.0 \times 1.0$  mm).

## Data Analysis

Data were processed using FieldTrip toolbox (Oostenveld et al., 2011) and graph theoretical analyses were carried out using the Brain Connectivity Toolbox (Rubinov and Sporns, 2010) in MATLAB R2016a (The Mathworks, Inc., Natick, MA, USA).

### Preprocessing and Response-Locked Analysis

The raw data were initially epoched from  $-900$  ms to  $1800$  ms relative to the onset of stimuli, and baseline corrected using the  $-900$  ms to  $0$  ms window. Line noise was attenuated at 60, 120, 180 Hz by means of a very sharp discrete Fourier transform filter, and bandpass filtered from 0.1 Hz to 100 Hz. Scanner jump artifacts were automatically identified (by means of a median filter) and rejected from trials. An average of  $3.1 \pm 3.8$  (mean  $\pm$  STD) trials were rejected across individuals. To minimize edge effects, we selected a wide initial window, free from overlap across trials/conditions. The baseline and active windows were subsequently defined as  $-400$  ms to  $0$  ms and  $600$ – $1000$  ms, respectively. In previous verb generation studies, researchers have documented strong beta-band *event related desynchrony* (ERD)  $\sim 300$ – $800$  ms following picture presentation (Kadis et al., 2008, 2011; Ressel et al., 2008; Pang et al., 2011). However, the use of audio stimuli in the

current study necessitates focusing on a later, active window (to account for the delay we shifted the “active” window out by 300 ms).

### Source Inversion

The covariance matrix, a key ingredient for source inversion, was computed from whole window (combined data epochs of  $[-400$  to  $0]$  and  $[600$ – $1000]$  ms), so called “common filter” for each subject and each condition. The common filter improves the source estimation (see Wibral et al., 2011; Haegens et al., 2014). Anatomical MR scans of subjects were segmented and tissue types (brain, skull and scalp surface) were extracted. MEG and MRI scans were coregistered using the common fiducial markers. Single shell head models were constructed from the segmented MRI (Nolte, 2003). A 3-D grid was constructed with a dipole resolution of 10 mm (spacing inside the brain), and the lead field computed for each grid point. To estimate time-series sources, a linearly constrained minimum-variance (LCMV) beamformer with 0.1% regularization was used (Van Veen et al., 1997). A differential beamformer analysis (mean power difference between active and baseline windows) was performed. We report source activations in the low-beta (13–23 Hz) band, to be consistent with literature (Kadis et al., 2008, 2011; Ressel et al., 2008; Pang et al., 2011). We performed a Monte Carlo test with 5000 randomizations, to identify significant ( $p < 0.05$ ) low-beta ERD for each individual. Statistics for each random reshuffling was computed by a paired/dependent-sample *t*-test and multiple comparisons were corrected with an FDR threshold value of  $q = 0.05$ . For visualization, we spatially normalized sources to a template brain in MNI space. The scaling of child and adolescent brains into adult template space is generally considered minimal (for example see Burgund et al., 2002).

### Connectivity Analysis

For connectivity analysis, time-series sources were estimated in a broadband (3–30 Hz) frequency range. Whole-brain connectivity patterns were assessed by computing the PLV for each voxel pair during both “active” (600–1000 ms following stimulus onset) and “baseline” ( $-400$  ms to  $0$  ms from stimulus onset) periods (Lachaux et al., 1999):  $PLV(\omega) = \left| \left\langle \sum e^{j\theta(\omega)} \right\rangle_N \right|$  where the phase difference  $\theta(\omega)$  was derived from Fourier transform of voxel timeseries across  $N$  trials. This metric was selected since we were interested in characterizing network maps based on the presence of connections, independent of the directionality of connections. We computed active minus the baseline window connectivity to isolate task-related effects.

### Network Analysis

A network analysis from the graph theory perspective was performed on the adjacency matrices. The adjacency matrices were binarized based on an arbitrary threshold of 0.7, corresponding to 70% maximum connectivity strength for each subject. Comparison of three arbitrary thresholds of 50, 70 and 90% applied to a network by EVC measure is shown in Supplementary Figure S1. To identify hubs, we computed three measures of centrality, including *degree*, *EVC* and *betweenness centrality*, as implemented in Brain Connectivity Toolbox

(Rubinov and Sporns, 2010). Most simply, network degree is the total number of suprathreshold connections at each node, EVC is an extension of degree (it assigns relative scores to the nodes based on their neighbors' degrees), and betweenness centrality is a tendency for a node to occupy positions along shortest paths (Freeman, 1977; Bonacich, 2007).

For a group analysis, an automated anatomical labeling (AAL) atlas (Tzourio-Mazoyer et al., 2002) consisting of 116 subdivisions of cortical, subcortical and cerebellar regions was used to combine mean network measures computed at voxel-level in each parcel. Group differences in network findings (i.e., hub strength) were assessed using an independent samples *t*-test (FDR with  $q = 0.05$ ).

To characterize hemispheric involvement, we derived a conventional laterality index,  $LI = (L - R)/(L + R)$ , for the EVC scores within all frontal and temporal lobe parcels (15 distinct anatomical regions per hemisphere). LI values greater than 0.25 were considered as left-lateralized, less than  $-0.25$  as right-lateralized, and intermediate values as a bilateral.

## RESULTS

The groups averaged sources revealed prominent beta (13–30 Hz) ERD in inferior frontal and posterior temporal regions i.e., Broca's and Wernicke's regions (**Figure 1A**). Voxel-wise and parcellated network maps indicate the importance of left perisylvian sites for language expression in both groups (**Figures 1B,C**, see Supplementary Figure S2 for parcellated maps of individuals).

Laterality indices based on EVC suggested a left-hemispheric dominance in 3/15 (20%) young children and 10/14 (71%) adolescents. Other subjects were either bilateral (10/15, or 66.6% of young children, and 4/14, or 28% of adolescents) or had right-hemisphere dominance (2/15, or 13.3% of young children). A boxplot of LI variations is shown in **Figure 2**, indicating a range of  $[-0.1952, 0.1428]$  and  $[-0.0896, 0.2773]$  for the young children and adolescents, respectively.

Network maps constructed from each of the centrality measures were generally consistent, showing predominant hubs in left prefrontal cortex. The pattern of hub distribution for degree and EVC were nearly identical; in contrast, the map derived from betweenness centrality was relatively focal to the left IFG (**Figure 3**). Visual analyses suggested a better consistency for EVC (than the other two measures) with the connectivity patterns demonstrated on a subject-wise basis; hence EVC was preferred for subsequent analyses and interpretations.

The parcellated maps for the group of young children suggested stronger hubs in right, rather than left hemisphere regions (**Figure 4A**). As summarized in **Table 1**, the EVC values for young children in the order of strength were, right Rolandic operculum, right Heschl's gyrus, right insula, right putamen, right inferior frontal operculum, right STG, left pars orbitalis, right pars triangularis and left STG. In comparison, group parcellated map of adolescents showed strong hubs in left perisylvian regions, right Heschl's gyrus (or primary auditory cortex) in STG area and bilateral subcortical regions (**Figure 4B**). Important ROIs in the order of

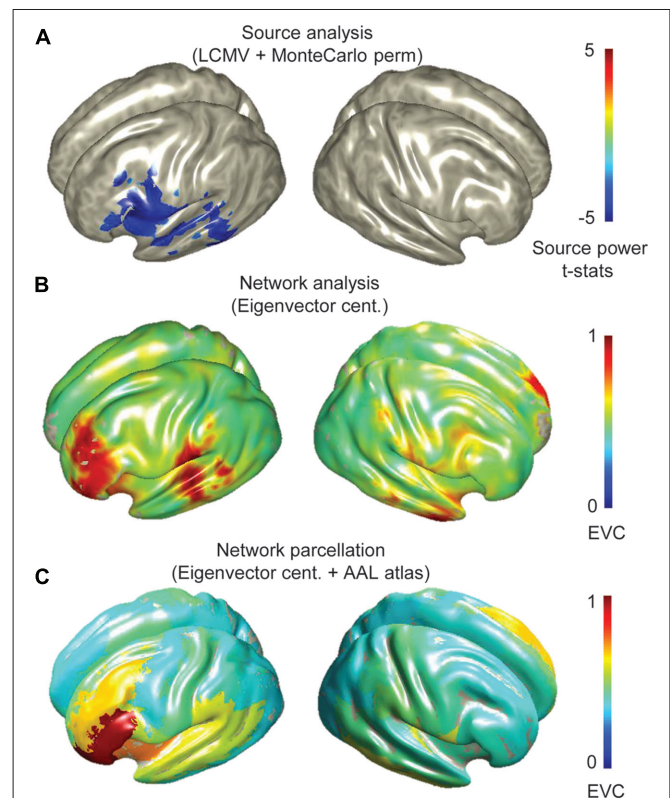


**FIGURE 1 | Group source and network analysis of all participants (14 adolescents and 15 children) during verb generation magnetoencephalography (MEG) experiment. (A)** Topographical map of grand averaged source activations from differential beamformer analyses and statistically validated by Monte Carlo simulations (permutation test with an alpha level of 0.05, 5000 randomizations and FDR correction with  $q = 0.05$  for multiple comparisons), showing beta event related desynchrony (ERD) in perisylvian regions. **(B)** Network maps captured by eigenvector centrality (EVC) at the voxel-level, and **(C)** parcellated EVC. Group average network measures were scaled between 0 and 1.

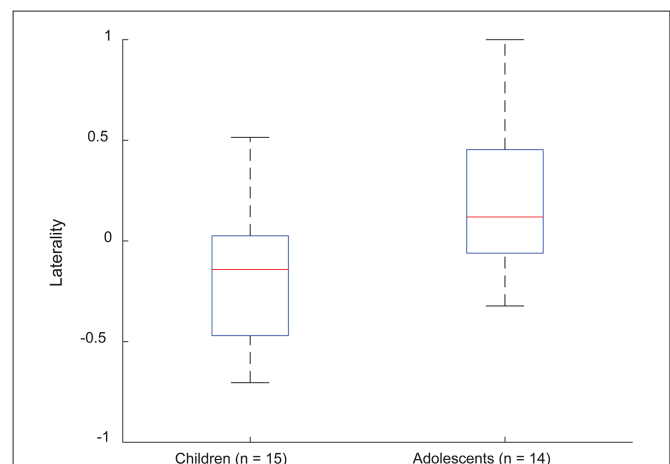
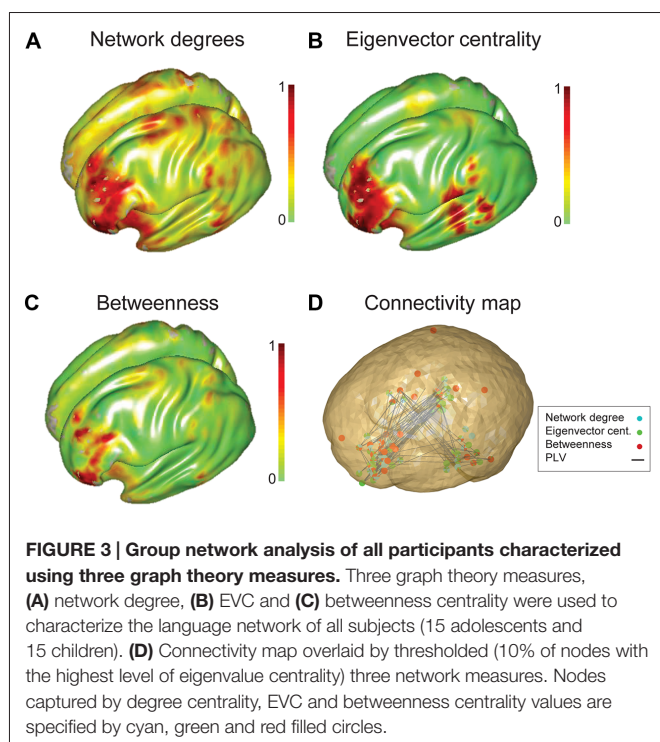


**FIGURE 2 | Laterality indices for EVC in frontotemporal parcels, for young children and adolescents performing verb generation.** Positivity and negativity correspond to left- and right-lateralized EVC distributions, respectively.



network strength were, right Rolandic operculum, right Heschl's gyrus, left amygdala, left globus pallidus, left putamen, left pars triangularis, left Heschl's gyrus, left pars orbitalis, left insula and left STG. Unlike the adolescent group, stronger hubs were found in right cortical and subcortical regions of children, as in **Figure 4A** and **Table 1**. This may support the hypothesis that right hemisphere supports language in very early childhood (Chiron et al., 1997; see "Discussion" Section). We also observed hubs in cerebellar regions of adolescents and not children, mainly at right cerebellar hemisphere (see **Figure 4**, not reported in **Table 1**). Overall, hubs identified for children were stronger in right frontotemporal cortical and subcortical regions, but weaker at the left prefrontal and cerebellar regions.

To evaluate the developmental changes, we compared group network differences between young children and adolescents. As shown in **Figures 5A,B** and are summarized in the last column of **Table 1**, significant ( $p < 0.05$ , FDR corrected) differences were found in right cerebellar regions as well as significant differences in a cortical region (left frontal inferior orbital) and a subcortical region (left putamen in basal ganglia). This may imply a significant role of cerebellar regions in developmental changes from childhood to adolescence (or adulthood), as discussed below.

## DISCUSSION

This is one of the first demonstrations of using large-scale connectivity and graph theoretical (network) analysis to identify hubs associated with language processing. Our

results are generally consistent with previous findings in terms of lateralization and localization in early development. Findings provide support for underlying dynamic topological organization of the pediatric language network.

Group source analysis showed low-beta [13, 23] Hz ERD at left inferior frontal and posterior temporal regions, consistent with previous MEG expressive language studies (Singh et al., 2002; Hirata et al., 2004; Kadis et al., 2008, 2011; Ressel et al., 2008; Pang et al., 2011; Doesburg et al., 2012). Whole brain connectivity based on PLV metric derived from broad-band (3–30 Hz) sources suggested prominent connectivity at left perisylvian sites (**Figure 1B**) and hubs in left prefrontal regions (**Figure 1C**).

Interestingly, we found stronger hubs in left prefrontal regions of the adolescents than the children (**Figure 4** and **Table 1**), including anterior regions of the IFG (pars orbitalis, or BA47). The developmental increase in left inferior frontal connectivity is consistent with recent studies of effective connectivity patterns in children performing verb generation (Kadis et al., 2015); the localization suggests a pivotal role of the anterior inferior frontal cortex for expressive language, involving regions that extend beyond canonical Broca's area.

The network analysis for the young children suggested bilateral hubs in cortical and subcortical language regions, but with stronger effects in the right hemisphere (**Figure 4A**). Such right hemispheric effects were clearly observed in the network contrast of young children against adolescents (**Table 1**). Previous findings based on changes in cerebral blood flow (dynamic SPECT) have demonstrated a right-dominance in infants and toddlers, with a subsequent shift toward the left after 3 years of age (Chiron et al., 1997). Our results support early right hemispheric effects, (see also **Table 1**).

Beyond the canonical language regions, our network analyses revealed strong hubs at subcortical regions, including the lentiform nuclei (putamen and globus pallidus), in both children and adolescents (see **Figure 4** and **Table 1**). Findings support the notion that both cortical and subcortical regions are critical for expressive language (Houk, 2005; Booth et al., 2007; Mestres-Missé et al., 2008). Others have indeed shown that subcortical regions, along with cortical-subcortical interactions, may play a critical role in a variety of language processes (Johnson and Ojemann, 2000; Wahl et al., 2008). Group network analyses revealed prominent hubs in the right cerebellum (**Figure 4**). Significant hubs were found in the same regions for the contrasted network of adolescents against young children (**Figure 5**). This may imply the importance of right cerebellum in generation of verbs as well as development of the expressive language network (Gabrieli et al., 1998; Middleton and Strick, 2000; Frings et al., 2006; Booth et al., 2007; Houk et al., 2007; Murdoch, 2010; Berl et al., 2014; Verly et al., 2014).

MEG permits recordings on the temporal scale of neuronal oscillations (ms) and fine spatial resolution (mm). A recent retinotopy mapping study has shown that MEG is able to estimate signals  $\sim 7$  mm in smooth regions of cortex and less than 1 mm for signals near curved gyri (Nasiotis et al., 2016). The high temporal and spatial resolution makes the MEG superior to fMRI for connectivity investigations, i.e., identifying

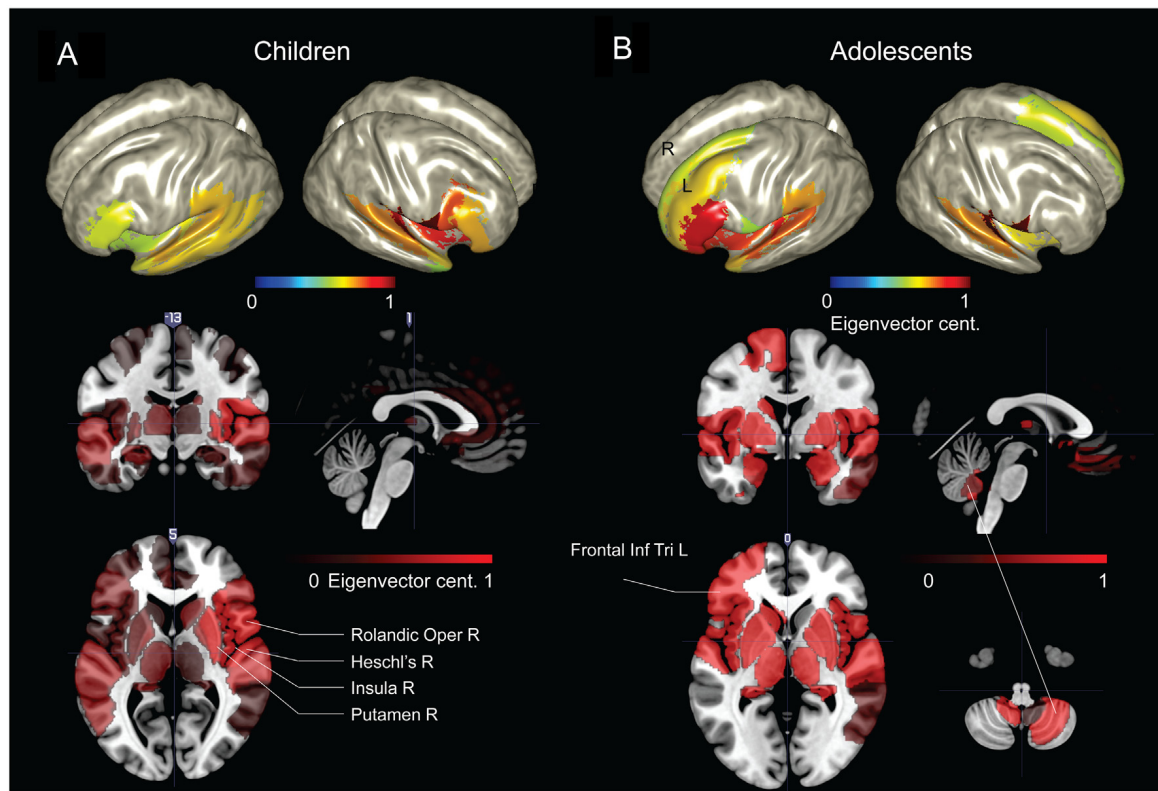


**FIGURE 4 | Group network-based parcellation of adolescents and children. (A)** Cortical and subcortical regions detected during group network analysis through EVC from children and **(B)** adolescents. Results have been thresholded with an arbitrary value of 0.7.

**TABLE 1 | Summary of regions of interest (ROIs) detected by network-based parcellated maps of two groups of subjects, adolescents and children.**

Children		Adolescents		Adolescents—Children		Children—Adolescents	
ROI	EVC (mean ± SE)	ROI	EVC (mean ± SE)	ROI	P (FDR)	ROI	P (FDR)
Rolandic Oper R	0.6 ± 0.02	Rolandic Oper R	0.56 ± 0.01	<b>Cerebellum 10 R</b>	0.0097	<b>Frontal Inf Tri R</b>	0.0026
Heschl R	0.56 ± 0.02	Heschl R	0.56 ± 0.01	<b>Cerebellum 8 R</b>	0.004	<b>Caudate R</b>	0.0037
Insula R	0.48 ± 0.01	Amygdala L	0.54 ± 0.02	<b>Frontal Inf Orb L</b>	0.045	<b>Frontal Inf Orb R</b>	0.088
Putamen R	0.47 ± 0.01	Pallidum L	0.52 ± 0.02	<b>Cerebellum 7b R</b>	0.0011	<b>Frontal Inf Oper R</b>	0.036
Frontal Inf Oper R	0.46 ± 0.01	Putamen L	0.51 ± 0.02	<b>Cerebellum 3 L</b>	0.028	<b>Olfactory R</b>	0.036
Temporal Sup R	0.43 ± 0.01	Frontal Inf Tri L	0.5 ± 0.02	Frontal Med Orb L	0.22	<b>Precentral L</b>	0.032
Frontal Inf Orb R	0.41 ± 0.02	Heschl L	0.47 ± 0.01	Putamen L	0.060	<b>Temporal Pole R</b>	0.030
Pallidum L	0.41 ± 0.02	Frontal Inf Orb L	0.45 ± 0.02	Amygdala L	0.23	<b>Cingulum Ant L</b>	0.026
Frontal Inf Tri R	0.41 ± 0.02	Insula L	0.45 ± 0.01	Frontal Inf Tri L	0.33	Insula R	0.060
Temporal Sup L	0.4 ± 0.01	Temporal Sup L	0.42 ± 0.01	Vermis 9	0.11	Cingulum Ant R	0.06

Significant ( $p < 0.05$ ) ROIs are specified in bold. Results are consistent with **Figures 4, 5**. EVC, Eigenvector centrality scaled between 0 and 1; SE, standard error; L, left hemisphere; R, right hemisphere; Orb, Orbital; Tri, Triangular; Oper, Operculum; Sup, Superior; Med, Medial; Inf, Inferior; Pallidum, globus pallidus.

interactions (temporally organized bursts) that occur within milliseconds, over millimeters (Bastos and Schoffelen, 2016). In pediatric studies, MEG is preferable because it offers less restrictive and less noisy testing environment than nMR. Yet, careful considerations are required in connectivity/network estimation; sensor-level connectivity will be inflated by common-source/mixing problems, and source localizations are inherently imperfect (inverse solution, underdetermined). However, the use of source analytic techniques that are robust to noise and correlated/coherent sources, and an understanding of the

limitations of both the inversion and connectivity metrics chosen, make MEG network analyses tenable (Schoffelen and Gross, 2009; Bastos and Schoffelen, 2016).

MEG has a lower sensitivity to subcortical sources due to complex cytoarchitecture of brain and the distance from sensors (Hillebrand and Barnes, 2002). Despite this challenge, many previous studies using both simulated and real data have successfully demonstrated estimates of subcortical generators e.g., in hippocampal and basal ganglia (David et al., 2011; Quraan et al., 2011; Mills et al., 2012; for a review see Attal et al., 2012).

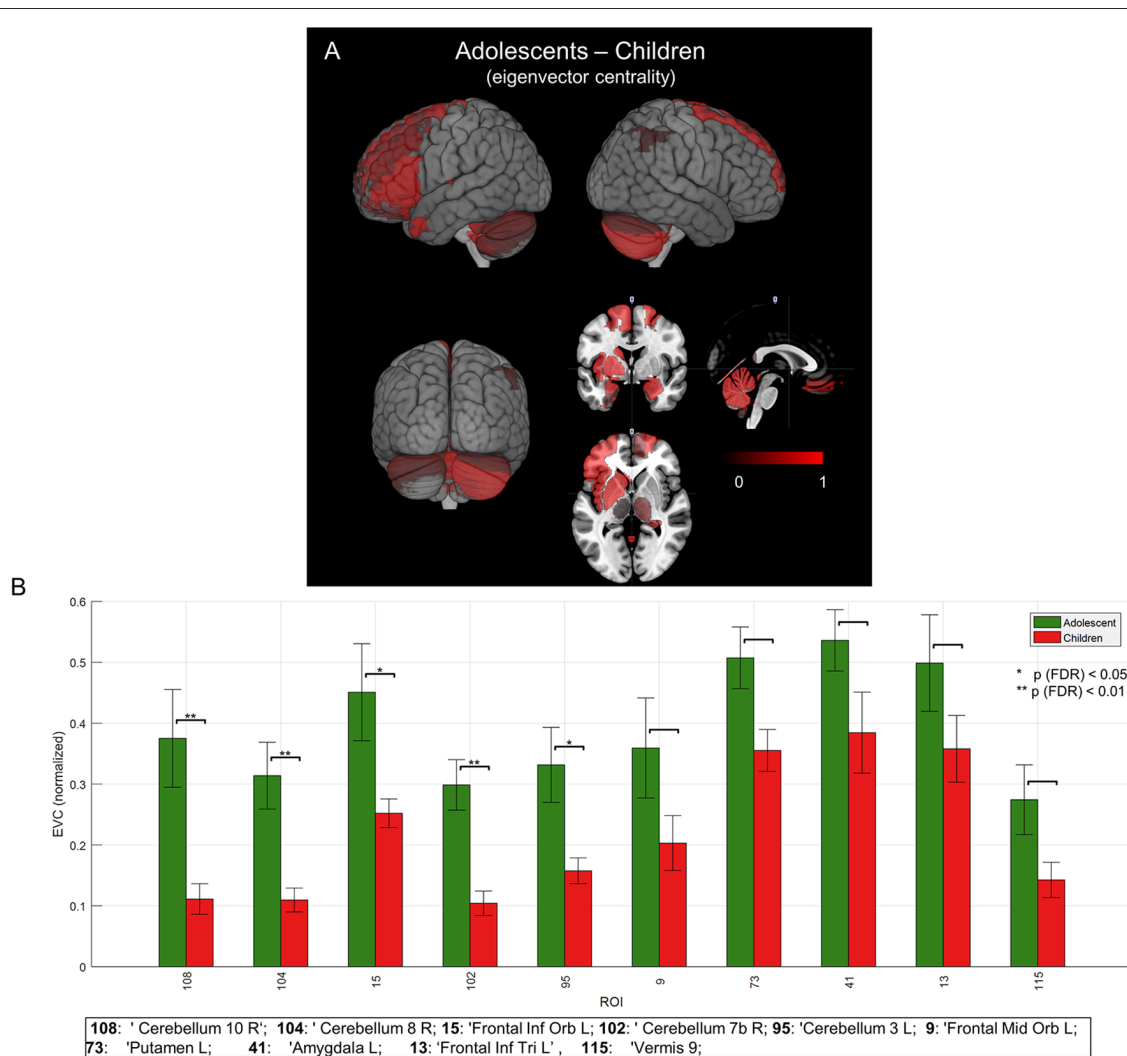


**FIGURE 5 | Mean group network-based parcellation difference between adolescent and children. (A)** Cortical (left inferior frontal gyrus (IFG)) and subcortical (left and right cerebellum) regions detected by group network difference between adolescents and children. **(B)** Regions of interests (ROIs) detected in group differences of adolescents and children. Error bars represent a standard error (SE). “\*” and “\*\*” represent  $p$  (FDR) < 0.05 and < 0.01, respectively.

To improve access to deep neuronal activity, we employed a semi-realistic single shell forward model by Nolte (2003), and a differential beamformer, which is less sensitive to background noise and do not underestimate deep sources (Quraan et al., 2011). Our subcortical findings are also in agreement, from two aspects, with a recent fMRI study on speech control (Fuertinger et al., 2015). First, they demonstrated the usefulness of the graph theoretical analysis in characterizing speech and language control network. Second, they detected communities (hubs) at prefrontal cortex and subcortical (insula, thalamus and putamen) and cerebellum regions. Yet, the subcortical estimates by MEG can be further evaluated using a realistic pseudo-MEG data wherein alternative forward and inverse modeling techniques can be conveniently used (Haufe and Ewald, 2016).

The current study shows that a whole brain connectivity and graph theoretical analysis of MEG data is powerful for

characterizing topological properties of the complex language network. The framework is sufficiently general to allow for application to other domain, also.

## AUTHOR CONTRIBUTIONS

DSK certifies that each of the authors made significant, intellectual contributions to this study and the development of the manuscript. VY conceptualized the methodological framework, and carried out the bulk of analyses for the current study. He prepared the initial manuscript, and carried out revisions after consulting with coauthors. BJW has been studying language models, and the potential for using graph theory metrics for identification of critical sites. BJW advised on graph analyses, choice of metrics and provided edits on the manuscripts during development. The work was carried out in DSK's laboratory, and was made possible through a

grant provided to DSK by the Research Institute at Cincinnati Children's Hospital Medical Center. DSK oversaw all aspects of the study, from conceptualization, recruitment, imaging, analyses and authorship of this manuscript.

## ACKNOWLEDGMENTS

This research was supported by a Trustee Award Grant received by DSK from the Cincinnati Children's Hospital Medical Center.

## REFERENCES

- Achard, S., and Bullmore, E. (2007). Efficiency and cost of economical brain functional networks. *PLoS Comput. Biol.* 3:e17. doi: 10.1371/journal.pcbi.0030017
- Allen, P., Mechelli, A., Stephan, K. E., Day, F., Dalton, J., Williams, S., et al. (2008). Fronto-temporal interactions during overt verbal initiation and suppression. *J. Cogn. Neurosci.* 20, 1656–1669. doi: 10.1162/jocn.2008.20107
- Attal, Y., Maess, B., Friederici, A., and David, O. (2012). Head models and dynamic causal modeling of subcortical activity using magnetoencephalographic/electroencephalographic data. *Rev. Neurosci.* 23, 85–95. doi: 10.1515/rns.2011.056
- Bassett, D. S., Bullmore, E. T., Meyer-Lindenberg, A., Apud, J. A., Weinberger, D. R., and Coppola, R. (2009). Cognitive fitness of cost-efficient brain functional networks. *Proc. Natl. Acad. Sci. U S A* 106, 11747–11752. doi: 10.1073/pnas.0903641106
- Bastos, A. M., and Schoffelen, J.-M. (2016). A tutorial review of functional connectivity analysis methods and their interpretational pitfalls. *Front. Syst. Neurosci.* 9:175. doi: 10.3389/fnsys.2015.00175
- Berl, M. M., Mayo, J., Parks, E. N., Rosenberger, L. R., VanMeter, J., Ratner, N. B., et al. (2014). Regional differences in the developmental trajectory of lateralization of the language network. *Hum. Brain Mapp.* 35, 270–284. doi: 10.1002/hbm.22179
- Binder, J. R., Frost, J. A., Hammeke, T. A., Cox, R. W., Rao, S. M., and Prieto, T. (1997). Human brain language areas identified by functional magnetic resonance imaging. *J. Neurosci.* 17, 353–362.
- Bitan, T., Booth, J. R., Choy, J., Burman, D. D., Gitelman, D. R., and Mesulam, M. M. (2005). Shifts of effective connectivity within a language network during rhyming and spelling. *J. Neurosci.* 25, 5397–5403. doi: 10.1523/JNEUROSCI.0864-05.2005
- Bitan, T., Burman, D. D., Lu, D., Cone, N. E., Gitelman, D. R., Mesulam, M. M., et al. (2006). Weaker top-down modulation from the left inferior frontal gyrus in children. *Neuroimage* 33, 991–998. doi: 10.1016/j.neuroimage.2006.07.007
- Bonacich, P. (2007). Some unique properties of eigenvector centrality. *Soc. Networks* 29, 555–564. doi: 10.1016/j.socnet.2007.04.002
- Booth, J. R., Wood, L., Lu, D., Houk, J. C., and Bitan, T. (2007). The role of the basal ganglia and cerebellum in language processing. *Brain Res.* 1133, 136–144. doi: 10.1016/j.brainres.2006.11.074
- Broca, P. (1861). Remarques sur le siège de la faculté du langage articulé suivies d'une observation d'aphémie. *Bull. Soc. Anthr.* 6, 330–357.
- Burgund, E. D., Kang, H. C., Kelly, J. E., Buckner, R. L., Snyder, A. Z., Petersen, S. E., et al. (2002). The feasibility of a common stereotactic space for children and adults in fMRI studies of development. *Neuroimage* 17, 184–200. doi: 10.1006/nimg.2002.1174
- Cao, F., Bitan, T., and Booth, J. R. (2008). Effective brain connectivity in children with reading difficulties during phonological processing. *Brain Lang.* 107, 91–101. doi: 10.1016/j.bandl.2007.12.009
- Chiron, C., Jambaque, I., Nabbout, R., Lounes, R., Syrota, A., and Dulac, O. (1997). The right brain hemisphere is dominant in human infants. *Brain* 120, 1057–1065. doi: 10.1093/brain/120.6.1057

We wish to acknowledge Claudio A. Toro-Serey and Cameron Laue Evans for their assistance with recruitment, assessment and data management.

## SUPPLEMENTARY MATERIAL

The Supplementary Material for this article can be found online at: <http://journal.frontiersin.org/article/10.3389/fnhum.2017.00173/full#supplementary-material>

- David, O., Maess, B., Eckstein, K., and Friederici, A. D. (2011). Dynamic causal modeling of subcortical connectivity of language. *J. Neurosci.* 31, 2712–2717. doi: 10.1523/JNEUROSCI.3433-10.2011
- Doesburg, S. M., Tingling, K., MacDonald, M. J., and Pang, E. W. (2015). Development of network synchronization predicts language abilities. *J. Cogn. Neurosci.* 28, 55–68. doi: 10.1162/jocn\_a\_00879
- Doesburg, S. M., Vinette, S. A., Cheung, M. J., and Pang, E. W. (2012). Theta-modulated gamma-band synchronization among activated regions during a verb generation task. *Front. Psychol.* 3:195. doi: 10.3389/fpsyg.2012.00195
- Fornito, A., Zalesky, A., and Breakspear, M. (2015). The connectomics of brain disorders. *Nat. Rev. Neurosci.* 16, 159–172. doi: 10.1038/nrn3901
- Freeman, L. C. (1977). A set of measures of centrality based on betweenness. *Sociometry* 40, 35–41. doi: 10.2307/3033543
- Friederici, A. D. (2011). The brain basis of language processing: from structure to function. *Physiol. Rev.* 91, 1357–1392. doi: 10.1152/physrev.00006.2011
- Friederici, A. D. (2012). The cortical language circuit: from auditory perception to sentence comprehension. *Trends Cogn. Sci.* 16, 262–268. doi: 10.1016/j.tics.2012.04.001
- Frings, M., Dimitrova, A., Schorn, C. F., Elles, H. G., Hein-Kropp, C., Gizewski, E. R., et al. (2006). Cerebellar involvement in verb generation: an fMRI study. *Neurosci. Lett.* 409, 19–23. doi: 10.1016/j.neulet.2006.08.058
- Fuertinger, S., Horwitz, B., and Simonyan, K. (2015). The functional connectome of speech control. *PLoS Biol.* 13:e1002209. doi: 10.1371/journal.pbio.1002209
- Gabrieli, J. D., Poldrack, R. A., and Desmond, J. E. (1998). The role of left prefrontal cortex in language and memory. *Proc. Natl. Acad. Sci. U S A* 95, 906–913. doi: 10.1073/pnas.95.3.906
- Haegens, S., Cousijn, H., Wallis, G., Harrison, P. J., and Nobre, A. C. (2014). Inter- and intra-individual variability in  $\alpha$  peak frequency. *Neuroimage* 92, 46–55. doi: 10.1016/j.neuroimage.2014.01.049
- Haufe, S., and Ewald, A. (2016). A simulation framework for benchmarking EEG-based brain connectivity estimation methodologies. *Brain Topogr.* doi: 10.1007/s10548-016-0498-y [Epub ahead of print].
- He, Y., and Evans, A. (2010). Graph theoretical modeling of brain connectivity. *Curr. Opin. Neurol.* 23, 341–350. doi: 10.1097/WCO.0b013e32833aa567
- Hillebrand, A., and Barnes, G. R. (2002). A quantitative assessment of the sensitivity of whole-head MEG to activity in the adult human cortex. *Neuroimage* 16, 638–650. doi: 10.1006/nimg.2002.1102
- Hirata, M., Kato, A., Taniguchi, M., Saitoh, Y., Ninomiya, H., Ihara, A., et al. (2004). Determination of language dominance with synthetic aperture magnetometry: comparison with the wada test. *Neuroimage* 23, 46–53. doi: 10.1016/j.neuroimage.2004.05.009
- Holland, S. K., Vannest, J., Mecoli, M., Jacola, L. M., Tillema, J., Karunanayaka, P. R., et al. (2007). Functional MRI of language lateralization during development in children. *Int. J. Audiol.* 46, 533–551. doi: 10.1080/14992020701448994
- Houk, J. C. (2005). Agents of the mind. *Biol. Cybern.* 92, 427–437. doi: 10.1007/s00422-005-0569-8

- Houk, J. C., Bastianen, C., Fansler, D., Fishbach, A., Fraser, D., Reber, P. J., et al. (2007). Action selection and refinement in subcortical loops through basal ganglia and cerebellum. *Philos. Trans. R. Soc. Lond. B Biol. Sci.* 362, 1573–1583. doi: 10.1098/rstb.2007.2063
- Johnson, M. D., and Ojemann, G. A. (2000). The role of the human thalamus in language and memory: evidence from electrophysiological studies. *Brain Cogn.* 42, 218–230. doi: 10.1006/brcg.1999.1101
- Kadis, D. S., Dimitrijevic, A., Toro-Serey, C. A., Smith, M. L., and Holland, S. K. (2015). Characterizing information flux within the distributed pediatric expressive language network: a core region mapped through fMRI-constrained MEG effective connectivity analyses. *Brain Connect.* 6, 76–83. doi: 10.1089/brain.2015.0374
- Kadis, D. S., Pang, E. W., Mills, T., Taylor, M. J., McAndrews, M. P., and Smith, M. L. (2011). Characterizing the normal developmental trajectory of expressive language lateralization using magnetoencephalography. *J. Int. Neuropsychol. Soc.* 17, 896–904. doi: 10.1017/S1355617711000932
- Kadis, D., Smith, M. L., Mills, T., and Pang, E. W. (2008). Expressive language mapping in children using MEG; MEG localization of expressive language cortex in healthy children: application to paediatric clinical populations. *Down Syndr. Q.* 10, 5–12.
- Karunanayaka, P. R., Holland, S. K., Schmithorst, V. J., Solodkin, A., Chen, E. E., Szafarski, J. P., et al. (2007). Age-related connectivity changes in fMRI data from children listening to stories. *Neuroimage* 34, 349–360. doi: 10.1016/j.neuroimage.2006.08.028
- Lachaux, J. P., Rodriguez, E., Martinerie, J., and Varela, F. J. (1999). Measuring phase synchrony in brain signals. *Hum. Brain Mapp.* 8, 194–208. doi: 10.1002/(SICI)1097-0193(1999)8:4<194::AID-HBM4>3.0.CO;2-C
- Leff, A. P., Schofield, T. M., Stephan, K. E., Crinion, J. T., Friston, K. J., and Price, C. J. (2008). The cortical dynamics of intelligible speech. *J. Neurosci.* 28, 13209–13215. doi: 10.1523/JNEUROSCI.2903-08.2008
- Lohmann, G., Hoehl, S., Brauer, J., Danielmeier, C., Bornkessel-Schlesewsky, I., Bahlmann, J., et al. (2010). Setting the frame: the human brain activates a basic low-frequency network for language processing. *Cereb. Cortex* 20, 1286–1292. doi: 10.1093/cercor/bhp190
- Mandelli, M. L., Vilaplana, E., Brown, J. A., Hubbard, H. I., Binney, R. J., Attygalle, S., et al. (2016). Healthy brain connectivity predicts atrophy progression in non-fluent variant of primary progressive aphasia. *Brain* 139, 2778–2791. doi: 10.1093/brain/aww195
- McIntosh, A. R., and Mišić, B. (2013). Multivariate statistical analysis for neuroimaging data. *Annu. Rev. Psychol.* 64, 499–525. doi: 10.1146/annurev-psych-113011-143804
- Mestres-Missé, A., Càmarà, E., Rodriguez-Fornells, A., Rotte, M., and Münte, T. F. (2008). Functional neuroanatomy of meaning acquisition from context. *J. Cogn. Neurosci.* 20, 2153–2166. doi: 10.1162/jocn.2008.20150
- Middleton, F. A., and Strick, P. L. (2000). Basal ganglia and cerebellar loops: motor and cognitive circuits. *Brain Res. Rev.* 31, 236–250. doi: 10.1016/s0165-0173(99)00040-5
- Mills, T., Lalancette, M., Moses, S. N., Taylor, M. J., and Quraan, M. A. (2012). Techniques for detection and localization of weak hippocampal and medial frontal sources using beamformers in MEG. *Brain Topogr.* 25, 248–263. doi: 10.1007/s10548-012-0217-2
- Murdoch, B. E. (2010). The cerebellum and language: historical perspective and review. *Cortex* 46, 858–868. doi: 10.1016/j.cortex.2009.07.018
- Nasiotis, K., Clavagner, S., Baillet, S., and Pack, C. C. (2016). High-resolution retinotopic maps estimated with magnetoencephalography. *Neuroimage* 145, 107–117. doi: 10.1016/j.neuroimage.2016.10.017
- Nolte, G. (2003). The magnetic lead field theorem in the quasi-static approximation and its use for magnetoencephalography forward calculation in realistic volume conductors. *Phys. Med. Biol.* 48, 3637–3652. doi: 10.1088/0031-9155/48/22/002
- Oostenveld, R., Fries, P., Maris, E., and Schoffelen, J. M. (2011). FieldTrip: open source software for advanced analysis of MEG, EEG and invasive electrophysiological data. *Comput. Intell. Neurosci.* 2011:156869. doi: 10.1155/2011/156869
- Pang, E. W., Wang, F., Malone, M., Kadis, D. S., and Donner, E. J. (2011). Localization of Broca's area using verb generation tasks in the MEG: validation against fMRI. *Neurosci. Lett.* 490, 215–219. doi: 10.1016/j.neulet.2010.12.055
- Pei, X., Leuthardt, E. C., Gaona, C. M., Brunner, P., Wolpaw, J. R., and Schalk, G. (2011). Spatiotemporal dynamics of electrocorticographic high  $\gamma$  activity during overt and covert word repetition. *Neuroimage* 54, 2960–2972. doi: 10.1016/j.neuroimage.2010.10.029
- Power, J. D., Schlaggar, B. L., Lessov-Schlaggar, C. N., and Petersen, S. E. (2013). Evidence for hubs in human functional brain networks. *Neuron* 79, 798–813. doi: 10.1016/j.neuron.2013.07.035
- Price, C. J. (2000). The anatomy of language: contributions from functional neuroimaging. *J. Anat.* 197, 335–359. doi: 10.1046/j.1469-7580.2000.19730335.x
- Quraan, M. A., Moses, S. N., Hung, Y., Mills, T., and Taylor, M. J. (2011). Detection and localization of hippocampal activity using beamformers with MEG: a detailed investigation using simulations and empirical data. *Hum. Brain Mapp.* 32, 812–827. doi: 10.1002/hbm.21068
- Ressel, V., Wilke, M., Lidzba, K., Lutzenberger, W., and Krägeloh-Mann, I. (2008). Increases in language lateralization in normal children as observed using magnetoencephalography. *Brain Lang.* 106, 167–176. doi: 10.1016/j.bandl.2008.01.004
- Rubinov, M., and Sporns, O. (2010). Complex network measures of brain connectivity: uses and interpretations. *Neuroimage* 52, 1059–1069. doi: 10.1016/j.neuroimage.2009.10.003
- Schoffelen, J.-M., and Gross, J. (2009). Source connectivity analysis with MEG and EEG. *Hum. Brain Mapp.* 30, 1857–1865. doi: 10.1002/hbm.20745
- Schofield, T. M., Iverson, P., Kiebel, S. J., Stephan, K. E., Kilner, J. M., Friston, K. J., et al. (2009). Changing meaning causes coupling changes within higher levels of the cortical hierarchy. *Proc. Natl. Acad. Sci. U S A* 106, 11765–11770. doi: 10.1073/pnas.0811402106
- Singh, K. D., Barnes, G. R., Hillebrand, A., Forde, E. M. E., and Williams, A. L. (2002). Task-related changes in cortical synchronization are spatially coincident with the hemodynamic response. *Neuroimage* 16, 103–114. doi: 10.1006/nimg.2001.1050
- Sonty, S. P., Mesulam, M.-M., Weintraub, S., Johnson, N. A., Parrish, T. B., and Gitelman, D. R. (2007). Altered effective connectivity within the language network in primary progressive aphasia. *J. Neurosci.* 27, 1334–1345. doi: 10.1523/JNEUROSCI.4127-06.2007
- Stam, C. J., de Haan, W., Daffertshofer, A., Jones, B. F., Manshanden, I., van Cappellen van Walsum, A. M., et al. (2009). Graph theoretical analysis of magnetoencephalographic functional connectivity in Alzheimer's disease. *Brain* 132, 213–224. doi: 10.1093/brain/awn262
- Supekar, K., Musen, M., and Menon, V. (2009). Development of large-scale functional brain networks in children. *PLoS Biol.* 7:e1000157. doi: 10.1371/journal.pbio.1000157
- Turken, A. U., and Dronkers, N. F. (2011). The neural architecture of the language comprehension network: converging evidence from lesion and connectivity analyses. *Front. Syst. Neurosci.* 5:1. doi: 10.3389/fnsys.2011.00001
- Tzourio-Mazoyer, N., Landeau, B., Papathanassiou, D., Crivello, F., Etard, O., Delcroix, N., et al. (2002). Automated anatomical labeling of activations in SPM using a macroscopic anatomical parcellation of the MNI MRI single-subject brain. *Neuroimage* 15, 273–289. doi: 10.1006/nimg.2001.0978
- Van Veen, B. D., van Drongelen, W., Yuchtman, M., and Suzuki, A. (1997). Localization of brain electrical activity via linearly constrained minimum variance spatial filtering. *IEEE Trans. Biomed. Eng.* 44, 867–880. doi: 10.1109/10.623056
- Verly, M., Verhoeven, J., Zink, I., Mantini, D., Peeters, R., Deprez, S., et al. (2014). Altered functional connectivity of the language network in ASD: role of classical language areas and cerebellum. *Neuroimage Clin.* 4, 374–382. doi: 10.1016/j.nicl.2014.01.008
- Wahl, M., Marzinzik, F., Friederici, A. D., Hahne, A., Kupsch, A., Schneider, G. H., et al. (2008). The human thalamus processes syntactic and semantic language violations. *Neuron* 59, 695–707. doi: 10.1016/j.neuron.2008.07.011

- Wernicke, C. (1874). *Der Aphasische Symptomencomplex. Eine Psychologische Studie Auf Anatomischer Basis, Wernicke's Work on Aphasia*. Breslau: M. Cohn & Weigert.
- Wibral, M., Rahm, B., Rieder, M., Lindner, M., Vicente, R., and Kaiser, J. (2011). Transfer entropy in magnetoencephalographic data: quantifying information flow in cortical and cerebellar networks. *Prog. Biophys. Mol. Biol.* 105, 80–97. doi: 10.1016/j.pbiomolbio.2010.11.006
- Xiao, Y., Friederici, A. D., Margulies, D. S., and Brauer, J. (2016). Development of a selective left-hemispheric fronto-temporal network for processing syntactic complexity in language comprehension. *Neuropsychologia* 83, 274–282. doi: 10.1016/j.neuropsychologia.2015.09.003

**Conflict of Interest Statement:** The authors declare that the research was conducted in the absence of any commercial or financial relationships that could be construed as a potential conflict of interest.

Copyright © 2017 Youssofzadeh, Williamson and Kadis. This is an open-access article distributed under the terms of the Creative Commons Attribution License (CC BY). The use, distribution or reproduction in other forums is permitted, provided the original author(s) or licensor are credited and that the original publication in this journal is cited, in accordance with accepted academic practice. No use, distribution or reproduction is permitted which does not comply with these terms.